PHYSICAL REVIEW C **79**, 035201 (2009)

Resonance energy of the $\bar{K}NN$-πYN system

Y. Ikeda[*] and T. Sato[†]
Department of Physics, Graduate School of Science, Osaka University, Toyonaka, Osaka 560-0043, Japan
(Received 8 September 2008; published 3 March 2009)

The resonance energies of strange dibaryons are investigated with the use of the $\bar{K}NN$-πYN coupled-channels Faddeev equation. It is found that the pole positions of the predicted three-body amplitudes are significantly modified when the three-body coupled-channels dynamics is approximated, as is done in the literature, by the effective two-body $\bar{K}N$ interactions.

DOI: 10.1103/PhysRevC.79.035201 PACS number(s): 13.75.Jz, 11.80.Jy, 11.30.Rd, 14.20.Pt

I. INTRODUCTION

Since the deeply bound kaonic nuclear states were predicted [1–3], the few-nucleon systems with strangeness have attracted increasing interest. It is generally believed that those states can be generated by an attractive interaction between a kaon and a nucleon in the isospin $I = 0$ channel. It has been suggested that the kaon-nucleon interaction may even modify the spatial distribution of nucleons in nuclei. Among the deeply bound kaonic states, the resonances in the $\bar{K}NN$-πYN ($Y = \Sigma, \Lambda$) system (strange dibaryon resonance) are particularly interesting because the three-hadron dynamics involved can be handled accurately with the use of the well-established Faddeev equation. This also means that the study of this strange dibaryon system will provide us with information on the nature of the $\bar{K}N$-$\pi\Sigma$ interaction and the basic mechanism of the kaon-nucleus interactions.

The FINUDA Collaboration [4] reported a signature of the $\bar{K}NN$-πYN coupled-channels resonance below the $\pi\Sigma N$ threshold. The reported resonance has a binding energy $B \sim 115$ MeV and a width $\Gamma \sim 67$ MeV. However the interpretation of the signal is still open to discussion [5]. More information on the $\bar{K}NN$-πYN resonance is expected to become available from Spring-8 and J-PARC in the near future. The first theoretical prediction of the resonance energy was given in Ref. [2]. Using a variational approach and a phenomenological $\bar{K}N$-$\pi\Sigma$ potential, it was found that the binding energy and the width of the $\bar{K}NN$-πYN system are $(B, \Gamma) \sim (48, 60)$ MeV. The calculation in Ref. [6], which used a $\bar{K}N$ interaction generated from a chiral unitary model, gave $(B, \Gamma) \sim (20, 40 \sim 70)$ MeV. In both of these earlier works, the three-body $\bar{K}NN$-πYN coupled-channels problem was handled with the use of effective $\bar{K}N$ interactions obtained by truncating the Fock space into $\bar{K}NN$. Meanwhile, the three-body dynamics can be fully taken into account with the use of the Faddeev formulation, and a study based on the Faddeev formulation was presented by the present authors [7] and by Shevchenko *et al.* [8]. Reference [7], which employed the $\bar{K}N$-$\pi\Sigma$ interaction based on the leading order chiral Lagrangian, gave $(B, \Gamma) \sim (60 \sim 95, 45 \sim 80)$ MeV, while Ref. [8], which adopted a phenomenological $\bar{K}N$ interaction, reported $(B, \Gamma) \sim (50 \sim 70, 100)$ MeV. Thus, at present, theoretical predictions on the resonance energy spread over a rather wide range [2,6–11].

A major uncertainty in theoretically estimating the resonance energy of the $\bar{K}NN$-πYN system is that an accurate description of the $\bar{K}N$ interaction including its off-shell behavior is still missing; this is particularly true for the energy region below the $\bar{K}N$ threshold. Taking a reverse viewpoint, we may hope that there is a possibility to constrain $\bar{K}N$ dynamics from the study of the $\bar{K}NN$-πYN resonance. To achieve this goal, however, it is crucial to treat the three-body dynamics as accurately as possible in a theoretical calculation for a given $\bar{K}N$ model.

In most of the existing theoretical work, the resonance energy is predicted to lie below the $\bar{K}NN$ threshold and above the $\pi\Sigma N$ threshold; thus the relevant state is a continuum (localized) state in the $\pi\Sigma N(\bar{K}NN)$ Fock space. In this circumstance it is an inviting idea to work in the $\bar{K}NN$ subspace by eliminating the $\pi\Sigma N$ states [2,6,12], and many analyses in the literature adopt this "effective potential approach" and introduce effective $\bar{K}N$ interactions to subsumethe effects of the eliminated channel. One thing to be emphasized here is that, when the Fock space is truncated, the resulting effective interaction in a subspace in general becomes a many-body operator, but that this fundamental feature is ignored in the existing effective potential treatments, which only consider effective two-body $\bar{K}N$ interactions. In this connection, it seems worth noting that the Faddeev approach [7,8], which fully takes account of coupled-channels three-body dynamics, tends to give a binding energy deeper than that of the approximate effective potential approach.

In this article we present a detailed examination of the nature of the approximations involved in the existing effective potential approach calculations. (For convenience, the approximate effective potential approach in question will be simply referred to as EPA). It turns out (see below) that, starting from the full coupled-channels Faddeev equations, we can simulate the EPA by introducing certain simplifying assumptions regarding the two-body t matrix embedded in the three-body system. This allows us to scrutinize the nature of approximations involved in the EPA in relation to the full Faddeev calculation [7] and to assess the validity (or limitation)

[*]ikeda@kern.phys.sci.osaka-u.ac.jp
[†]tsato@phys.sci.osaka-u.ac.jp

 ©2009 The American Physical Society

of the EPA. For this assessment, we focus here on comparison of the resonance positions obtained with the EPA and with the full calculation.

A comment is in order here concerning methods used to determine the resonance energy. In the present article we determine the resonance energy from the position of a pole in the scattering amplitude, as explained in detail in Ref. [7]. Recently, it has been suggested [13] that a pole in the complex energy plane may not adequately characterize a resonance. According to Ref. [13], as the strength of the $\bar{K}N$ interaction is artificially increased, the trajectory of the pole moves below the $\pi\Sigma$ threshold, but keeping a finite width (signature for a virtual state; see, however, Ref. [14]). We address here this question as well and show that the problem of a pole moving to a virtual state for the three-body amplitude is an artifact of the approximation used in the EPA.

In Sec. II, we briefly explain the method we use for solving the Faddeev equation for the coupled $\bar{K}NN \oplus \pi YN (Y = \Sigma, \Lambda)$ system, and we elucidate what approximations are involved in going from the full Faddeev formulation to the EPA. Section III is devoted to the explanation of how the $\bar{K}N$-πY interactions used in our calculations are derived from the chiral Lagrangian. The numerical results on the predicted resonance energies are presented in Sec. IV, and Sec. V gives a summary.

II. COUPLED-CHANNEL APPROACH FOR $\bar{K}NN$-πYN SYSTEM

A. AGS equation and resonance pole

The Faddeev equation for a three-particle system with separable two-body interactions can be cast into the Alt-Grassberger-Sandhas (AGS) equation [15],

$$X_{i,j}(\vec{p}_i, \vec{p}_j, W) = (1-\delta_{i,j})Z_{i,j}(\vec{p}_i, \vec{p}_j, W) + \sum_{n\neq i}\int d\vec{p}_n Z_{i,n}(\vec{p}_i, \vec{p}_n, W)\tau_n(W)X_{n,j}(\vec{p}_n, \vec{p}_j, W), \quad (1)$$

where W is the total scattering energy and $X_{i,j}(\vec{p}_i, \vec{p}_j, W)$ with $i, j = 1, 2, 3$ are the scattering amplitudes. The channel i (j) is characterized by the spectator particle i (j). For example, $i = 1$ represents a quasi two-body channel in which the particle 1 is the spectator of the last interaction between particles 2 and 3. The momentum of the spectator particle i and the relative momentum for channel i are denoted by $\vec{p}_i$ and $\vec{q}_i$, respectively.

The driving term $Z_{i,j}(\vec{p}_i, \vec{p}_j, W)$ of the AGS equation is given by the particle exchange interaction illustrated in Fig. 1(a) and can be written as

$$Z_{i,j}(\vec{p}_i, \vec{p}_j, W) = \frac{g_i^*(\vec{q}_i)g_j(\vec{q}_j)}{W - E_i(\vec{p}_i) - E_j(\vec{p}_j) - E_k(-\vec{p}_i - \vec{p}_j) + i\epsilon}. \quad (2)$$

Here we used the two-body interaction for channel i of the following form

$$\langle\vec{q}_i'|v_i|\vec{q}_i\rangle = \gamma_i g_i(\vec{q}_i')g_i(\vec{q}_i). \quad (3)$$

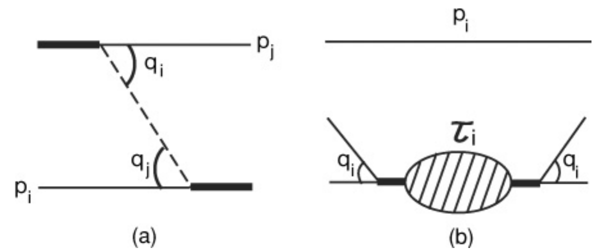

FIG. 1. Graphical representation of (a) one-particle-exchange interaction $Z_{i,j}(\vec{p}_i, \vec{p}_j, W)$ and (b) two-body t matrix $\tau_i(W)$. The relative momentum of the interacting particles is denoted by $\vec{q}_i$ for the spectator particle i.

The "isobar" propagator τ_i, illustrated in Fig. 1(b), is given by

$$(\tau_i(W))^{-1} = 1/\gamma_i - \int d\vec{q}_i \frac{|g_i(\vec{q}_i)|^2}{W - E_i(\vec{p}_i) - E_{jk}(\vec{p}_i, \vec{q}_i) + i\epsilon}. \quad (4)$$

Here $E_{jk}(\vec{p}_i, \vec{q}_i) = \sqrt{(E_j(\vec{q}_i) + E_k(\vec{q}_i))^2 + \vec{p}_i^2}$ is the energy of the interacting particles (j and k) expressed in terms of the relative momentum $\vec{q}_i$ and the momentum of the spectator particle $\vec{p}_i$. The isobar propagator τ_i, which is a part of the two-body t matrix within the three-particle system is further examined in the next section.

In this work we investigate a strange dibaryon resonance with angular momentum $J^\pi = 0^-$ and isospin $I = 1/2$. The main Fock-space components of the resonance are $\bar{K}NN$ and $\pi\Sigma N$ states that couple with each other through the $I = 0$ $\bar{K}N$-$\pi\Sigma$ interaction. We also take into account the $\pi\Lambda N$ component, which couples with the main $\bar{K}N$-$\pi\Sigma$ components through the $I = 1$ $\bar{K}N$-πY interaction. The AGS equation then becomes coupled-channels equations involving the channels $\bar{K}NN$ ($\bar{K}N_{I=0}$, $\bar{K}N_{I=1}$, $NN_{I=1}$), $\pi\Sigma N$($\pi N_{I=1/2}$, $\pi N_{I=3/2}$, $\pi\Sigma_{I=0}$, $\pi\Sigma_{I=1}$), and $\pi\Lambda N$ ($\pi N_{I=1/2}$, $\pi\Lambda_{I=1}$). We assume that all the orbital angular momenta are s waves. After isospin-angular momentum projection and the antisymmetrization of the two nucleons, Eq. (1) becomes the following coupled integral equation [16,17],

$$X_{\alpha,\beta}(p', p, W) = C^1_{\alpha,\beta}Z_{\alpha,\beta}(p', p, W) + \sum_{\gamma,\delta}\int dq q^2 C^2_{\alpha,\gamma}Z_{\alpha,\gamma}(p', q, W)\tau_{\gamma,\delta}(W)X_{\delta,\beta}(q, p, W). \quad (5)$$

Here α, β are specified by the Fock space of the three particles and the quantum number of the interacting pair. The coefficients $C^{1,2}_{\alpha,\beta}$ are the spin-isospin recoupling coefficients given in Ref. [7].

The energy of the strange dibaryon resonance is determined by searching for a pole in the scattering amplitude X. To this end, the amplitude is analytically continued to the unphysical sheet by choosing an appropriate path of momentum integration, and then a pole in the amplitude is located using the eigenvalue of the kernel $Z\tau$ in the above equation (see Refs. [7,18–22]).

B. Approximate treatment of three-body dynamics

In the AGS equation, the three-particle dynamics is incorporated in the particle exchange mechanism Z and the propagator τ. The former is the three-body interaction and the latter is determined by the two-body t matrix in the presence of a spectator particle. We first examine how the two-body t matrix in the three-body system differs from that in a free space. The t matrix of $\bar{K}N$-$\pi\Sigma$ scattering in the three-particle system is described by the following KNN-$\pi Y\Sigma$ coupled-channels equation,

$$t_{\alpha,\beta}(W) = v_{\alpha,\beta} + \sum_{\gamma} v_{\alpha,\gamma} G_0^{\gamma N}(W) t_{\gamma,\beta}(W), \quad (6)$$

where $\alpha, \beta, \gamma = \bar{K}N$ and $\pi\Sigma$, and the Green function is

$$G_0^{\alpha N}(W) = \frac{1}{W - E_N(\vec{p}_N) - \sqrt{(E_{M_\alpha}(\vec{q}) + E_{B_\alpha}(\vec{q}))^2 + \vec{p}_N^{\,2}} + i\epsilon}. \quad (7)$$

Here $\vec{p}_N$ is the momentum of the spectator nucleon and $\vec{q}$ is the relative momentum of meson (M_α) and baryon (B_α) in the center of mass system of the channel α. The spectator momentum shifts the effective scattering energy from $W - m_N$ to $W - E_N(p)$ and modifies the on-shell momentum of the $\pi\Sigma N$ scattering state. One therefore expects that the motion of the spectator plays an important role in calculating the binding energy and width of the resonance.

The isobar propagator $\tau_{\alpha,\beta}(W)$ in Eq. (5) is related to the above t matrix as

$$\langle \vec{q}_\alpha | t_{\alpha,\beta}(W) | \vec{q}_\beta \rangle = g_\alpha(\vec{q}_\alpha) \tau_{\alpha,\beta}(W) g_\beta(\vec{q}_\beta). \quad (8)$$

Note that $\tau_{\alpha,\beta}(W)$ depends on the momentum of the spectator nucleon through the three-body Green function in Eq. (7). Clearly, the effects of the spectator motion on $\tau_{\alpha,\beta}(W)$ depend on the momentum distribution of the spectator nucleon, which can be determined only by solving three-body dynamics.

As mentioned, in the EPA the three-body problem is treated within the $\bar{K}NN$ Fock space. To make contact with the EPA, we rewrite Eq. (6) by eliminating the $\pi\Sigma N$ state, which results in the introduction of the effective interaction $v_{\rm eff}$. Thus

$$t_{\bar{K}N\text{-}\bar{K}N}(W) = v_{\rm eff}(W, \vec{p}_N) + v_{\rm eff}(W, \vec{p}_N) G_0^{\bar{K}NN}(W) t_{\bar{K}N\text{-}\bar{K}N}(W). \quad (9)$$

The effective interaction $v_{\rm eff}$ is defined by

$$v_{\rm eff}(W, \vec{p}_N) = v_{\bar{K}N\text{-}\bar{K}N} + v_{\bar{K}N\text{-}\pi\Sigma} G_0^{\pi\Sigma N}(W) \times (1 + \bar{t}_{\pi\Sigma-\pi\Sigma}(W) G_0^{\pi\Sigma N}(W)) v_{\pi\Sigma-\bar{K}N}, \quad (10)$$

$$\bar{t}_{\pi\Sigma-\pi\Sigma}(W) = v_{\pi\Sigma-\pi\Sigma} + v_{\pi\Sigma-\pi\Sigma} G_0^{\pi\Sigma N}(W) \bar{t}_{\pi\Sigma-\pi\Sigma}(W). \quad (11)$$

Note that $\bar{t}$ involves only rescattering through the $\pi\Sigma$ interaction. Solving the above set of equations is still equivalent to solving the original Faddeev equation. The difficulty of treating the three-body continuum ($\pi\Sigma N$) is hidden in the effective potential $v_{\rm eff}$, which is a three-body interaction that depends on the momentum of the spectator nucleon through the Green function.

A drastic simplification of $v_{\rm eff}$ can be achieved by neglecting the momentum dependence of the spectator or, more explicitly, by approximating the $\pi\Sigma N$ Green function, $G_0^{\pi\Sigma N}(W)$, in Eqs. (10) and (11) with

$$G_{0,\rm approx}^{\pi\Sigma N}(W) = \frac{1}{W - m_N - E_\pi(\vec{q}) - E_\Sigma(\vec{q}) + i\epsilon}. \quad (12)$$

This approximate treatment of the three-body dynamics represents the EPA as derived from the Faddeev formalism.

III. MODEL OF $\bar{K}N$ INTERACTION

We use here the models developed in our previous work [7] for describing the πN, $\bar{K}N$-$\pi\Sigma$-$\pi\Lambda$, and NN interactions. Here we briefly explain the $\bar{K}N$-$\pi\Sigma$ interaction in the $I = 0$ s-wave channel, which plays a crucial role in our study of the strange dibaryons. Our starting point is the following leading order effective chiral Lagrangian for a baryon ψ_B and a pseudoscalar meson ϕ,

$$L_{\rm int} = \frac{i}{8F_\pi^2} \mathrm{Tr}\,(\bar{\psi}_B \gamma^\mu [[\phi, \partial_\mu \phi], \psi_B]). \quad (13)$$

The s-wave meson-baryon potential derived from $L_{\rm int}$ is of the following separable form

$$\langle \vec{p}', \beta | V_{\rm BM} | \vec{p}, \alpha \rangle = -C_{\beta,\alpha} \frac{1}{(2\pi)^3 8F_\pi^2} \frac{m_\beta + m_\alpha}{\sqrt{4E_\beta(\vec{p}')E_\alpha(\vec{p})}} \times g_\beta(\vec{p}') g_\alpha(\vec{p}), \quad (14)$$

with $g_\alpha(\vec{p}) = \Lambda_\alpha^4/(\vec{p}^2 + \Lambda_\alpha^2)^2$. Here $\vec{p}$ and $\vec{p}'$ are the momenta of the mesons in the initial α and the final β states, respectively. The coupling constants $C_{\beta,\alpha}$ are $C_{\bar{K}N\text{-}\bar{K}N} = 6$, $C_{\bar{K}N\text{-}\pi\Sigma} = -\sqrt{6}$, and $C_{\pi\Sigma-\pi\Sigma} = 8$. Thus the potential is attractive for both $\bar{K}N$ and $\pi\Sigma$ channels. The strength of the potential at zero momentum is determined by the pion decay constant $F_\pi (F_\pi = 92.4$ MeV). We found only one resonance in the $I = 0$ $\bar{K}N$-$\pi\Sigma$ s-wave channel. Meanwhile it has been shown in Refs. [12,23,24] that two resonance poles may exist in this channel. The potential in Eq. (14) is independent of the scattering energy. The energy dependence of the $\bar{K}N$-$\pi\Sigma$ interactions is one of the important features that differentiate our approach from the chiral unitary approach. The properties of the resonances and the energy dependence of the potentials in the s-wave meson-baryon scattering will be examined in Ref. [25].

We first discuss the values of the cutoff parameters, Λ_α's, to be used in this work. Table I gives two sets of choices, Model (A) in the first row and Model (B) in the second row. The cutoff parameters for Model (A) are taken from Model (f) in Ref. [7], which was constructed to generate a resonance

TABLE I. The cutoff parameters and the resonance energy of the $\Lambda(1405)$.

	$\Lambda_{\bar{K}N}$ (MeV)	$\Lambda_{\pi\Sigma}$ (MeV)	Resonance energy (MeV)
(A)	1160	1100	$1405.8 - i25.2$
(B)	1100	1100	$1414.2 - i18.6$

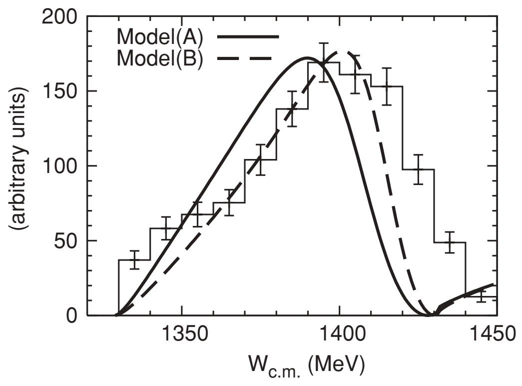

FIG. 2. Invariant mass distribution of the $\pi\Sigma$.

at around 1405 MeV [26]. When the couplings between the $\bar{K}N$ and the $\pi\Sigma$ are switched off in Model (A), a bound state appears in the $\bar{K}N$ channel and there is no resonance in the $\pi\Sigma$ channel. To test the prediction of Model (A) in the energy region below the $\bar{K}N$ threshold, we study the $\pi^-\Sigma^+$ mass distribution in the K^-p reaction [27]. Following Ref. [28], we calculate the $\pi^-\Sigma^+$ mass distribution from the $I = 0$ $\pi\Sigma$ scattering t matrix

$$\frac{dN}{dW_{\text{c.m.}}} = C|t_{\pi\Sigma-\pi\Sigma}|^2 p_{\text{c.m.}}, \tag{15}$$

where $p_{\text{c.m.}}$ is the $\pi\Sigma$ relative momentum in the center of mass system. Because of the presence of an arbitrary constant C, only the shape of the mass distribution can be compared with the data. We assume that the mass distribution of $\pi^-\Sigma^+$ is dominated by the $I = 0$ amplitude and that the mass distribution can be deduced from the $\pi\Sigma$ rescattering, neglecting other energy dependence due to the $\pi\Sigma$ production mechanism. The mass distribution calculated from Model (A) is compared with the data in Fig. 2. Model (A) gives a spectrum slightly larger than the data in the lower mass region. To examine the model dependence of this analysis, we study Model (B), which gives a slightly better description of the $\pi^-\Sigma^+$ mass distribution. The results for Model (B) are shown as the dashed line in Fig. 2. Model (B) has a $\bar{K}N$ interaction slightly weaker than that of Model (A) because of the smaller value of the cutoff parameter. The resonance generated from Model (B) is less bound and has a narrower width than that generated from Model (A). Both models give a satisfactory

TABLE II. The pole energy of the strange dibaryon resonance is given in MeV. The pole energy is related to the binding energy B and the width Γ as $W_{\text{pole}} - m_K - 2m_N = -B - i\Gamma/2$.

	Model (A)	Model (B)
Full calculation	$-63.3 - i22.2$	$-44.4 - i22.8$
Without pion-exchange Z	$-66.9 - i21.7$	$-47.4 - i25.0$

description of the total cross sections for the $K^-p \to K^-p$ reaction [Fig. 3(a)], the $K^-p \to \pi^+\Sigma^-$ reaction [Fig. 3(b)], and the $K^-p \to \pi^-\Sigma^+$ [Fig. 3(c)] reaction.

IV. RESULTS AND DISCUSSION

The energies of the strange dibaryon resonances obtained from our Faddeev approach described in Sec. II are listed in the first row of Table II. The half width of the resonance is about 22 MeV [23 MeV] for Model (A)[(B)]. Model (B) gives a binding energy $(-B = \text{Re}\,(W_{\text{pole}}) - m_K - 2m_N)$ about 20 MeV smaller than that of Model (A).

In all of the previous theoretical studies of strange dibaryon resonances except our previous work [7], the $\pi\Sigma N$ Fock space is not treated explicitly; it is only included in the intermediate states of the two-body $\bar{K}N$-$\pi\Sigma$ scattering amplitude. The influence of this simplification can be examined in our approach by turning off the pion exchange Z term in Eq. (1). As can be seen in Table II, the pion-exchange Z term plays only a minor role in the determination of the resonance energy. In the following discussion therefore we will treat the Faddeev calculation without the pion-exchange Z term as the "Exact" calculation.

Table III provides comparisons between the resonance energy obtained in the Exact calculation and that obtained from the EPA described in Sec. II. Clearly, there are significant differences between the two approaches. The EPA calculation gives a binding energy 15 to 25 MeV smaller than that of the Exact calculation. Similar effects of the three-body dynamics were partly studied in Ref. [11]. To understand these results, it is informative to plot $\tau(W)$ defined in Eq. (4) as a function of the momentum p_N of the spectator nucleon in the most important $I = 0$ $\bar{K}N$ channel (see Fig. 4). The amplitude $\tau(W)$ is evaluated at $B = 66.9(47.4)$ MeV for Model (A)[(B)]. The

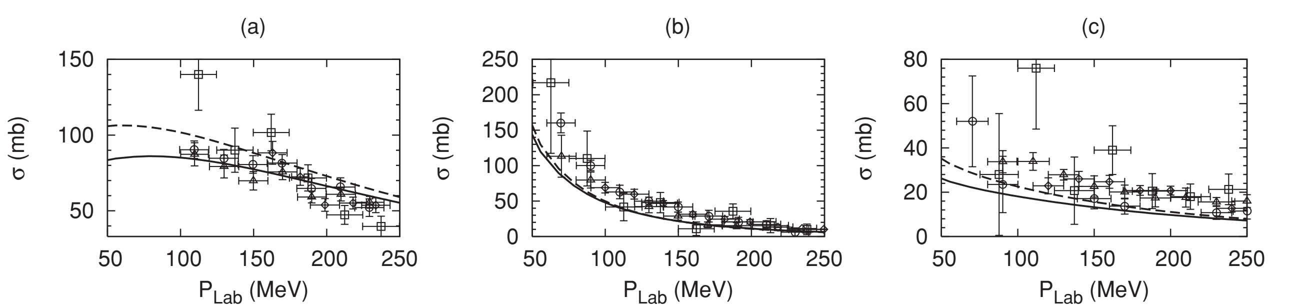

FIG. 3. The total cross sections of (a) $K^-p \to K^-p$, (b) $K^-p \to \pi^+\Sigma^-$, and (c) $K^-p \to \pi^-\Sigma^+$ reactions. The solid curves show cross sections calculated using Model (A); the dashed curves show cross sections calculated using Model (B). Data are taken from Refs. [29–33].

TABLE III. The pole energies obtained from EPA are compared with the Exact results; for an explanation of the term "Exact," see the text.

	Model (A)	Model (B)
Exact	$-66.9 - i21.7$	$-47.4 - i25.0$
EPA	$-41.8 - i35.4$	$-31.5 - i26.3$

real and imaginary parts of τ are shown in solid (dash-dotted) and dashed (dotted) curves for the Exact (EPA) calculations. As p_N increases, the scattering energy available for the $\pi\Sigma$ system decreases. This implies that in the Exact calculation the effects of the $\pi\Sigma$ threshold appear as a cusp in the real part of τ at threshold and the vanishing of the imaginary part of τ for the larger value of p_N (see Fig. 4). On the other hand, the EPA fails to capture this important behavior of the t matrix.

As mentioned, the EPA involves the approximation of the $\pi\Sigma N$ Green function. If we further approximate the $\bar{K}NN$ Green function we are led to the $t\rho$ approximation, which underlies the first order optical potential model. With this additional approximation we find a resonance at $(-67.4 - i64.2)$ MeV and $(-60.6 - i47.7)$ MeV for Models (A) and (B), respectively. We note that the additional approximation influences the resonance width drastically.

In summary, our analysis clearly shows that the exact treatment of three-body dynamics, such as given by the Faddeev formulation, is essential in making precise predictions on the resonance positions of the strange dibaryons.

Finally, we examine the behavior of the resonance pole trajectory as the magnitude of the $\bar{K}N$ interaction is artificially increased from its physical value. Let f stand for an enhancement factor of strength of the $I = 0$ $\bar{K}N$ interaction:

$$\bar{v}_{\bar{K}N,\bar{K}N} = f v_{\bar{K}N,\bar{K}N}. \tag{16}$$

The resonance determined from the pole of the scattering amplitude in our $\bar{K}N$-$\pi\Sigma$ coupled-channels model becomes a "virtual state" as f increases. This behavior of the two-body resonance pole is similar to the one observed in Ref. [13]. Although it was discussed in Ref. [13] that the spectrum shape of the Green function cannot be well explained based on the pole of the Green function, we emphasize that the spectrum shape can in fact be well described in terms of the resonance pole in the amplitude, we take into account the residue at the pole and the next order term in the Laurent expansion of the Green function (see Ref. [34]).

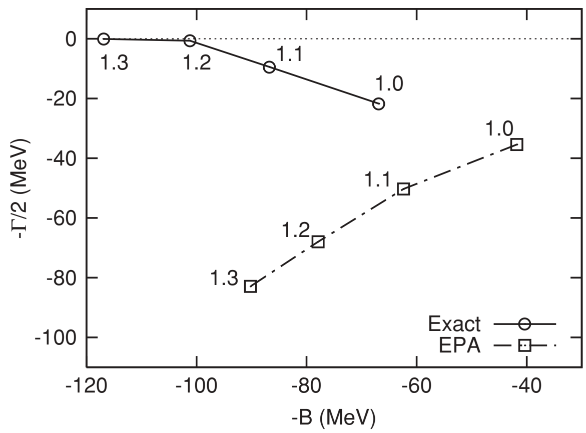

FIG. 5. Resonance energy of $\bar{K}NN$-πYN system for Model (A). The circles (squares) show resonance energies obtained with the Exact (EPA) treatment of the three-body Green function. The numbers attached to the circles and squares give the corresponding values of the enhancement factor f in Eq. (16).

The trajectory of the resonance pole occurring in the three-body system behaves quite differently from the resonance pole in the two-body system. The resonance energies obtained from our Model (A) are shown as circles in Fig. 5. The squares in the same figure correspond to the EPA results. The numbers attached to the circles and squares give the corresponding values of the enhancement factor f. As f increases, the binding energy of the resonance increases for both the Exact and the EPA cases. In the Exact calculation (circles), the imaginary part of the resonance energy becomes smaller as the binding energy increases and, for $f = 1.3$, the resonance almost becomes a bound state. On the other hand, in the EPA case (squares) the resonance becomes a virtual state as f grows. By contrast, in the Exact case the resonance energy of the three-body system determined from the pole of the scattering amplitude does not become a virtual state even for an (artificially) strong strong $\bar{K}N$ interaction. Here again we see

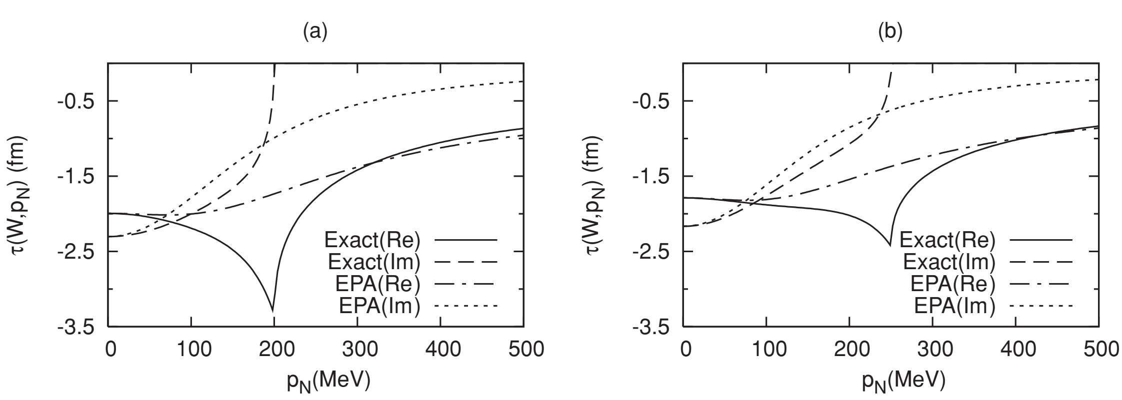

FIG. 4. $\bar{K}N$ amplitude of (a) Model (A) and (b) Model (B). $\bar{K}N$ amplitudes for $I = 0$ are shown for Exact and EPA treatments of the $\pi\Sigma N$ Green function.

the importance of taking a full account of three-body dynamics for understanding the strange dibaryon resonances.

V. SUMMARY

We have demonstrated the importance of taking a proper account of three-body dynamics in predicting the resonance energies of strange dibaryons. Within the Faddeev formulation we have examined the approximations involved in the existing effective potential approach (which for short we refer to as EPA). Upon eliminating the $\pi\Sigma N$ Fock space, the effective interaction in the $\bar{K}NN$ subspace becomes a three-body interaction that depends on the resonance energy and the momenta of all the three particles. We have shown that this energy and momentum dependence (which is neglected in the EPA) plays an important role in determining the resonance energies. As regards the behavior of the resonance position as a function of the strength of the $\bar{K}N$ potential, we have shown that the appearance of a virtual state in the EPA as the strength of the $\bar{K}N$ potential grows is an artifact of the approximations involved in the EPA. We have demonstrated that the results obtained from the Faddeev approach indicate that the resonance becomes a bound state as the $\bar{K}N$ potential becomes strong. In conclusion, we emphasize that a full treatment of three-body dynamics is essential in understanding the $\bar{K}NN$-πYN coupled-channels resonance.

ACKNOWLEDGMENTS

The authors thank Drs. T.-S. H. Lee and N. Suzuki for critical discussions on the resonance pole. The authors thank Professor K. Kubodera for reading the manuscript and making useful suggestions. This work is supported by the Japan Society for the Promotion of Science, Grant-in-Aid for Scientific Research(c) 20540270.

[1] Y. Akaishi and T. Yamazaki, Phys. Rev. C **65**, 044005 (2002).
[2] T. Yamazaki and Y. Akaishi, Phys. Lett. **B535**, 70 (2002).
[3] A. Dote, H. Horiuchi, Y. Akaishi, and T. Yamazaki, Phys. Rev. C **70**, 044313 (2004).
[4] M. Agnello *et al.*, Phys. Rev. Lett. **94**, 212303 (2005).
[5] V. K. Magas, E. Oset, A. Ramos, and H. Toki, Phys. Rev. C **74**, 025206 (2006).
[6] A. Dote, T. Hyodo, and W. Weise, Nucl. Phys. **A804**, 197 (2008); A. Dote, T. Hyodo, and W. Weise, Phys. Rev. C **79**, 014003 (2009).
[7] Y. Ikeda and T. Sato, Phys. Rev. C **76** 035203 (2007); Y. Ikeda and T. Sato, arXiv:nucl-th/0701001.
[8] N. V. Shevchenko, A. Gal, and J. Mares, Phys. Rev. Lett. **98**, 082301 (2007); N. V. Shevchenko, A. Gal, J. Mares, and J. Revai, Phys. Rev. C **76**, 044004 (2007).
[9] A. Arai, M. Oka, and S. Yasui, Prog. Theor. Phys. **119**, 103 (2008).
[10] T. Nishikawa and Y. Kondo, Phys. Rev. C **77**, 055202 (2008).
[11] S. Wycech and A. M. Green, Phys. Rev. C **79**, 014001 (2009).
[12] T. Hyodo and W. Weise, Phys. Rev. C **77**, 035204 (2008).
[13] Y. Akaishi, K. S. Myint, and T. Yamazaki, Proc. Jpn. Acad. Ser, B **84**, 264 (2008).
[14] A. Cieply and A. Gal, arXiv:0809.0422 [nucl-th].
[15] E. O. Alt, P. Grassberger, and W. Sandhas, Nucl. Phys. **B2**, 167 (1967).
[16] I. R. Afnan and A. W. Thomas, in *Modern Three-Hadron Physics*, edited by A. W. Thomas (Springer, Berlin, 1977), Chap. 1.
[17] I. R. Afnan and A. W. Thomas, Phys. Rev. C **10**, 109 (1974).
[18] W. Glöckle, Phys. Rev. C **18**, 564 (1978).
[19] A. Matsuyama and K. Yazaki, Nucl. Phys. **A534**, 620 (1991); A. Matsuyama, Phys. Lett. **B408**, 25 (1997).
[20] B. C. Pearce and I. R. Afnan, Phys. Rev. C **30**, 2022 (1984).
[21] I. R. Afnan and B. F. Gibson, Phys. Rev. C **47**, 1000 (1993).
[22] Y. V. Orlov and V. V. Turovtsev, Sov. Phys. JETP **59**, 934 (1984).
[23] D. Jido *et al.*, Nucl. Phys. **A725**, 181 (2003).
[24] A. Cieply and J. Smejkal, Eur. Phys. J. A **34**, 237 (2007).
[25] Y. Ikeda, H. Kamano, and T. Sato (in preparation).
[26] R. H. Dalitz and A. Deloff, J. Phys. G **17**, 289 (1991).
[27] R. J. Hemingway, Nucl. Phys. **B253**, 742 (1985).
[28] E. A. Veit, B. K. Jennings, A. W. Thomas, and R. C. Barrett, Phys. Rev. D **31**, 1033 (1985).
[29] W. E. Humphrey and R. R. Ross, Phys. Rev. **127**, 1305 (1962).
[30] M. Sakitt *et al.*, Phys. Rev. **139**, B719 (1965).
[31] J. K. Kim, Phys. Rev. Lett. **14**, 29 (1965).
[32] W. Kittel, G. Otter, and I. Wacek, Phys. Lett. **21**, 349 (1966).
[33] D. Evans *et al.*, J. Phys. G **9**, 885 (1983).
[34] N. Suzuki, T. Sato, and T.-S. H. Lee, Phys. Rev. C **79**, 025205 (2009).